Clim Dyn (2013) 41:1439–1452
DOI 10.1007/s00382-012-1518-6

Importance of oceanic resolution and mean state on the extra-tropical response to El Niño in a matrix of coupled models

Andrew Dawson · Adrian J. Matthews · David P. Stevens · Malcolm J. Roberts · Pier Luigi Vidale

Received: 11 June 2012 / Accepted: 1 September 2012 / Published online: 16 September 2012

Abstract The extra-tropical response to El Niño in configurations of a coupled model with increased horizontal resolution in the oceanic component is shown to be more realistic than in configurations with a low resolution oceanic component. This general conclusion is independent of the atmospheric resolution. Resolving small-scale processes in the ocean produces a more realistic oceanic mean state, with a reduced cold tongue bias, which in turn allows the atmospheric model component to be forced more realistically. A realistic atmospheric basic state is critical in order to represent Rossby wave propagation in response to El Niño, and hence the extra-tropical response to El Niño. Through the use of high and low resolution configurations of the forced atmospheric-only model component we show that, in isolation, atmospheric resolution does not significantly affect the simulation of the extra-tropical response to El Niño. It is demonstrated, through perturbations to the SST forcing of the atmospheric model component, that biases in the climatological SST field typical of coupled model configurations with low oceanic resolution can account for the erroneous atmospheric basic state seen in these coupled model configurations. These results highlight the importance of resolving small-scale oceanic processes in producing a realistic large-scale mean climate in coupled models, and suggest that it might may be possible to "squeeze out" valuable extra performance from coupled models through increases to oceanic resolution alone.

Keywords North Pacific · Extra-tropical SST · ENSO · GCM · Basic state

A. Dawson · A. J. Matthews · D. P. Stevens
School of Mathematics, University of East Anglia, Norwich, UK

Present Address:
A. Dawson (✉)
Atmospheric, Oceanic and Planetary Physics, Department of Physics, University of Oxford, Oxford, UK
e-mail: dawson@atm.ox.ac.uk

A. J. Matthews
School of Environmental Sciences, University of East Anglia, Norwich, UK

M. J. Roberts
Met Office Hadley Centre, Exeter, UK

P. L. Vidale
Department of Meteorology, National Centre for Atmospheric Science, University of Reading, Reading, UK

1 Introduction

The coupled models used for the Intergovernmental Panel on Climate Change (IPCC) fourth assessment report (AR4; Randall et al. 2007) represent the current state-of-the-art in coupled climate modelling. The typical horizontal resolutions of these models is 2° in the atmospheric component and 1°–2° in the oceanic component. Systematic errors in simulating mean climate and its variability affect many coupled models of typical AR4 resolution. It is common for AR4 models to have an equatorial Pacific cold tongue that is too equatorially confined and extends too far into the western tropical Pacific. This implies an unrealistic simulation of coupled heat transfer mechanisms, such as tropical instability waves (TIWs; Philander et al. 1986), in the tropics. The appearance of a persistent inter-tropical convergence zone (ITCZ) south of the equator in the eastern and central equatorial Pacific in addition to the observed ITCZ north of the equator, (the ITCZ problem; Mechoso et al. 1995), is also common in AR4 models. This

systematic error in simulating the mean climate in the tropical Pacific affects the location of the Walker circulation and the simulation of El Niño.

Increased horizontal resolution in coupled climate models has typically improved the fidelity of climate simulations (e.g., Gordon et al. 2000; Pope and Stratton 2002; Johns et al. 2006). There is mounting evidence that resolving smaller scale processes, down to scales as small as the oceanic mesoscale, in coupled climate models can improve their ability to realistically represent large-scale mean climate and its variability. Roberts et al. (2004) showed that increasing the ocean resolution of the UK Met Office coupled general circulation model (GCM) in its HadCM3 configuration to $^1/_3^\circ$ resulted in many improvements in the simulation of oceanic circulation. More recently Shaffrey et al. (2009) showed that the coupled GCM HiGEM, with high horizontal resolution in both the atmosphere (1.25° longitude × 0.875° latitude) and the ocean ($^1/_3^\circ$), allows ocean–atmosphere coupling to occur on small spatial scales. In particular the interactions between the atmosphere and TIWs in the Pacific Ocean is realistically captured in the high resolution version, compared to the lower resolution configuration (HadGEM; 1.875° longitude × 1.25° latitude atmosphere, $1–^1/_3^\circ$ ocean). Shaffrey et al. (2009) also noted that the split ITCZ problem is reduced in HiGEM compared with that in HadGEM, a model of typical AR4 resolution. Roberts et al. (2009) showed that resolving TIWs in the Pacific Ocean can result in a reduced equatorial cold tongue bias.

For coupled models to be used for both long and short term climate prediction, they must be able to accurately represent climate variability. El Niño is one of the major modes of global climate variability, and an accurate representation of El Niño requires an accurate representation of the extra-tropical SST response, in addition to realistic tropical SST anomalies. Extra-tropical SSTs are important in the climate system, with SST gradients influencing the location of mid-latitude storm tracks (Norris 2000; Inatsu et al. 2002; Brayshaw et al. 2008, 2011). Deser and Blackmon (1995) used empirical orthogonal function (EOF) analysis of observed winter SST anomalies to understand North Pacific El Niño teleconnections. Their EOF 1 pattern is a canonical representation of the spatial distribution of El Niño SST anomalies in both the tropical Pacific and the extra-tropical North Pacific.

Extra-tropical SST anomalies during El Niño are generated by a teleconnection mechanism, often referred to as the atmospheric bridge. Convection anomalies in the tropical Pacific are caused by the anomalous tropical SST anomalies during El Niño. These convection anomalies lead to anomalous divergence and associated anomalous vorticity in the upper troposphere. This anomalous vorticity drives atmospheric Rossby waves that affect global atmospheric circulation. This large-scale atmospheric teleconnection alters the surface energy balance in the extra-tropics, due to a combination of surface wind speed anomalies and changes in near surface temperature and humidity affecting sensible and latent heat fluxes (Deser and Blackmon 1995; Alexander et al. 2002; Dawson et al. 2011).

A common problem in AR4 models is the inability to accurately simulate the temporal variation of SSTs during El Niño, with variability generally occurring on time scales faster than observed (AchutaRao and Sperber 2002). It has been shown that high resolution in the atmosphere component of a coupled model can improve the representation of El Niño, in particular the temporal SST variability in the tropics (Guilyardi et al. 2004; Navarra et al. 2008). However, Navarra et al. (2008) also showed that increased atmospheric resolution alone was unable to eliminate the systematic westward shift of El Niño SST anomalies that are common in AR4 coupled models. Shaffrey et al. (2009) found that the simulation of tropical El Niño SST anomalies is improved in integrations of HiGEM. The ability of HiGEM to simulate TIWs improves the representation of mean climate, which in turn improves the simulation of El Niño.

Dawson et al. (2011) showed that the extra-tropical response to El Niño in a coupled model with horizontal resolution typical of the IPCC AR4 simulations (HadGEM) has serious errors, and that a higher resolution configuration of the same model (HiGEM) has a much improved response that is similar to observations. It was shown that an unrealistic representation of the atmospheric basic state in the lower resolution model altered Rossby wave propagation characteristics, which ultimately causes the atmospheric teleconnection mechanism controlling extra-tropical SSTs during El Niño to be represented inaccurately. However, the cause of the errors in the basic state were not explained.

In this paper we will further the results of Dawson et al. (2011) by examining the underlying reasons why the high resolution coupled model HiGEM performs more realistically than the low resolution HadGEM with respect to the extra-tropical response to El Niño. We will determine whether it is in the atmospheric or oceanic component of the coupled system that increased horizontal resolution provides the best improvement, and determine the physical mechanisms that cause the unrealistic atmospheric basic state in the low resolution HadGEM configuration. A controlled examination into the effect of horizontal resolution in the oceanic and atmospheric components of the coupled model system is undertaken using a "matrix" of coupled model resolutions as in Roberts et al. (2009).

This paper is organized as follows: Sect. 2 describes the model configurations, data sets, and analysis methods used.

Table 1 Horizontal resolution (longitude × latitude) of atmosphere and ocean components of model configurations

Configuration	Atmosphere	Ocean
HiGEM	1.25° × 0.83°	$\frac{1}{3}^\circ \times \frac{1}{3}^\circ$
HadGEM	1.875° × 1.25°	1° × 1°[a]
LoHi	1.875° × 1.25°	$\frac{1}{3}^\circ \times \frac{1}{3}^\circ$
HiLo	1.25° × 0.83°	1° × 1°[a]
HiGAM	1.25° × 0.83°	–
HadGAM	1.875° × 1.25°	–

[a] Increasing to $\frac{1}{3}^\circ$ meridionally near the equator

Section 3 describes results from analysing the extra-tropical response to El Niño in a matrix of coupled and atmosphere-only model configurations. Section 4 then describes the results from atmosphere-only SST perturbation experiments. Section 5 provides a summary and conclusions from this work.

2 Data and methods

A matrix of coupled model resolutions consisting of four configurations is used in this study. The models are based on the Hadley Centre Global Environmental Model version 1 (HadGEM1), a configuration of the Met Office's Unified Model that is described fully in Johns et al. (2006). The configurations used are: a high resolution coupled model (HiGEM), a low resolution coupled model (HadGEM), a configuration with a low resolution atmosphere and a high resolution ocean (LoHi), and a configuration with a high resolution atmosphere and a low resolution ocean (HiLo). These models are as described in Roberts et al. (2009) and are earlier versions of the models used in the study of Dawson et al. (2011). The atmospheric components of the HiGEM and HadGEM models are also studied in atmosphere-only configurations (HiGAM and HadGAM respectively), forced by observed SSTs.

The horizontal resolution of the model configurations are summarised in Table 1. The horizontal resolution of HadGEM is typical of the state-of-the-art coupled model simulations used for the IPCC AR4. The physics and parameterizations are essentially the same in HiGEM and HadGEM, with the major differences in the oceanic component where high horizontal resolution has necessitated modifications to the subgrid-scale mixing parameterizations. This allows for a relatively clean comparison between model resolutions.

Two observational data sets are used in this study. Gridded sea surface temperature (SST) data are from the UK Met Office HadISST data set (Rayner et al. 2003). All other gridded fields are from the National Centers for Environmental Prediction/National Center for Atmospheric Research (NCEP/NCAR) reanalysis project (Kalnay et al. 1996).

For this study all data fields are first averaged into individual November to March (NDJFM) seasonal means. This reflects the tendency for the effects of El Niño to be more pronounced during boreal winter (Philander 1990). The length of the season is chosen so as to capture not only El Niño anomalies in the tropics, but also the extra-tropical response produced by teleconnections from the tropics. A sampling period of 50 NDJFM seasons is used for the observed data set. The size of this sampling period is constrained by the amount of reliable observed SST data available (1957/58 to 2006/07 inclusive). The sampling period for each of the models varies due to differing lengths of the integrations. In the case of coupled models, there is a significant adjustment period during the first 20 years of integration. This period is removed and the following years are used for this analysis. For HiGEM/HadGEM the sample period is model years 21–70 and for LoHi/HiLo the sample period is model years 21–50. The atmosphere-only integrations do not experience a significant adjustment time hence the sample period is model years 1–20, which uses boundary forcing from the period 1982 to 2001. All anomalies are relative to the full NDJFM mean. In this paper we compare the shorter 20-year atmosphere-only integrations to diagnostics from observations obtained by sampling a 50-year period. However, we note that the same conclusions are found when comparing these integrations to an appropriate 20-year sub-sample (1982–2001) of observations.

Regression maps are used throughout this study, following Kiladis and Weickmann (1992). The index used for all regression maps is an area average of SST in the region 178°W–106°W, 6°S–6°N (as in Dawson et al. 2011). This area captures the core variability of El Niño. This index will be referred to as the Equatorial Pacific (EP) index from here on. Regression maps represent the anomaly in response to a 1 °C change in the EP SST index.

Empirical orthogonal function (EOF) analysis is used to examine SST variability. In this paper, EOF 1 is presented as the correlation of the principal component (PC) time series associated with EOF 1 and the data time series at each grid point. This is a measure of the spatial localization of the co-varying part between the NDJFM Pacific SST anomaly and its primary mode of temporal variability, in effect showing the areas in which the observed or modelled SST varies in the same way as the pattern of EOF 1. Significance is determined by a Student's t test using the Fisher Z transformation (Wilks 2006). The critical correlation coefficients at the 95 % level for $N = 50$ and $N = 30$ degrees of freedom are $r_* = 0.278$ and $r_* = 0.360$ respectively.

3 The extra-tropical response to El Niño in a matrix of coupled models

The representation of the extra-tropical response to El Niño in the matrix of coupled models and the atmosphere-only configurations is now studied. The framework of the atmospheric bridge teleconnection mechanism introduced in Dawson et al. (2011) is used to gain insight into where in the coupled system horizontal resolution is most important.

3.1 Upper tropospheric response

Regression maps of 200 hPa vorticity anomaly for NDJFM are shown in Fig. 1. These show the upper tropospheric circulation anomalies associated with El Niño. Over the Pacific and North American regions, the anomaly pattern in the high resolution coupled model HiGEM (Fig. 1a) is very similar to observations (Fig. 1i). However, in the low resolution coupled model HadGEM (Fig. 1b) the anomaly pattern is different to observations, with weaker positive vorticity anomalies over the North Pacific and North America being shifted westward. The negative vorticity anomaly over Canada is present but shifted so as to be over the North East Pacific. Dawson et al. (2011) found that this shift of upper level circulation anomalies ultimately resulted in an erroneous extra-tropical SST response to El Niño.

In the LoHi configuration (Fig. 1c) the positive vorticity anomalies over the North Pacific and North America are similar to HiGEM, although the North Pacific anomaly is considerably stronger. Hence, it appears that the low resolution atmosphere is able to correctly simulate the atmospheric extra-tropical response to El Niño, if it is coupled to the high resolution ocean. In contrast, the HiLo configuration (Fig. 1d) has a pattern of vorticity anomalies that is very different to the observations. This strongly suggests that the dynamics of Rossby wave propagation in the HiLo configuration are not like those in the real atmosphere. These initial results from the cross-resolution models point to the importance of high resolution in the ocean, rather than the atmosphere, in correctly simulating the response to El Niño.

Vorticity regression maps are also shown for the atmosphere-only integrations forced by observed SSTs (HiGAM and HadGAM; Fig. 1e, f respectively). HiGAM and HadGAM have vorticity anomaly patterns that are similar to one another and to observations, with positive anomalies over the North Pacific and the southern USA and a negative anomaly over Canada. This is further evidence that the resolution of the HadGEM atmospheric component is not too low so as to prohibit an accurate representation of the extra-tropical response to El Niño, if it is forced by realistic (in this case observed) El Niño SST anomalies.

3.2 Atmospheric basic state

As in Dawson et al. (2011), we use the stationary Rossby wavenumber (K_s) diagnostic to examine the basic state through which Rossby waves propagate. This diagnostic is derived entirely from the time-mean zonal wind field $\bar{u}$ and is defined as

$$K_s = \left(\frac{\beta - \bar{u}_{yy}}{\bar{u}} \right)^{\frac{1}{2}}, \quad (1)$$

where β is the meridional planetary vorticity gradient, and $\bar{u}_{yy}$ is the time-mean meridional relative vorticity gradient (the contribution from the meridional wind component has been neglected). This diagnostic may be interpreted as a refractive index for Rossby waves, with waves refracted towards (away from) latitudes with higher (lower) values of K_s. Local maxima in K_s can therefore be interpreted as Rossby waveguides. We note that the refractive index interpretation depends on scale separation, with the scale of the (Rossby) waves being much smaller than the scale of variations in the basic state (Hoskins and Karoly 1981; Karoly 1983). Hoskins and Ambrizzi (1993) showed that even though these assumptions may not be strictly valid, the diagnostic and its refractive index interpretation is still qualitatively useful.

The atmospheric basic state in HiGEM (Fig. 2a) is dynamically similar to the observed basic state (Fig. 2i). There is a waveguide (maximum in stationary wavenumber) associated with the Asian-Pacific jet extending out across the Pacific. Over the central Pacific this waveguide merges with the waveguide associated with the North American jet entrance. This structure allows Rossby waves to propagate between the two waveguides, which Dawson et al. (2011) showed to be an important factor in simulating the extra-tropical response to El Niño.

In contrast, the stationary wavenumber map in HadGEM (Fig. 2b) shows a split waveguide structure over the North Pacific. The region of negative meridional vorticity gradient (dark hatching) centred at 30°N, 140°W dynamically separates the Pacific jet from the entrance to the North American jet, and will act as a barrier to Rossby wave propagation between the two. This structure was also noted in Dawson et al. (2011) for the low resolution coupled model and was determined to be the primary factor causing the erroneous extra-tropical response to El Niño in that model.

The LoHi configuration has a waveguide structure (Fig. 2c) that is much like HiGEM and the observations. This might be expected given the similar anomalous circulation (Fig. 1a, c) in HiGEM and the LoHi configuration. This is a considerable improvement over the HadGEM basic state. However, the atmospheric basic state in the

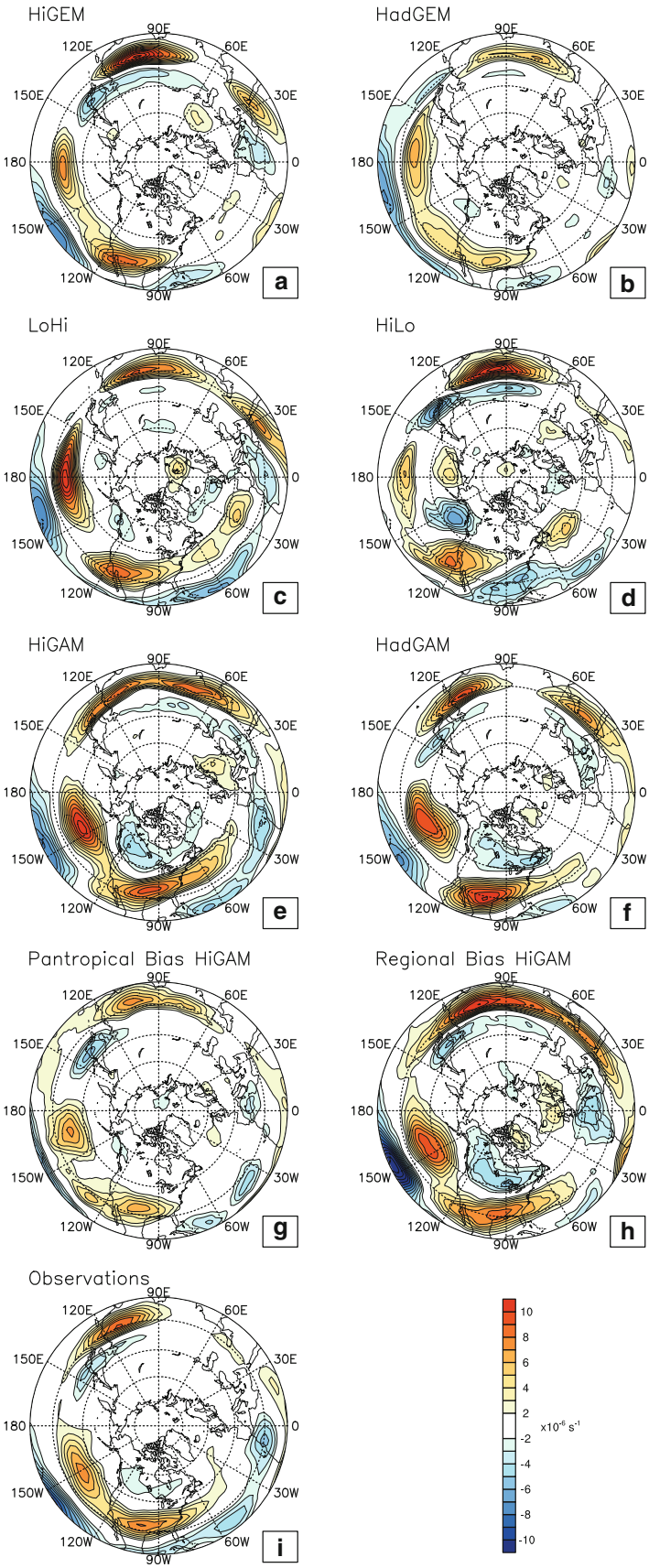

Fig. 1 Northern winter (NDJFM) 200 hPa vorticity anomaly associated with a 1 °C departure of the EP index. Contour interval is 10^{-6} s^{-1}. Contours between -2×10^{-6} and 2×10^{-6} s^{-1} are omitted. **a** HiGEM, **b** HadGEM, **c** LoHi, **d** HiLo, **e** HiGAM, **f** HadGAM, **g** pantropical bias HiGAM experiment, **h** regional bias HiGAM experiment, and **i** observations (NCEP/NCAR reanalysis)

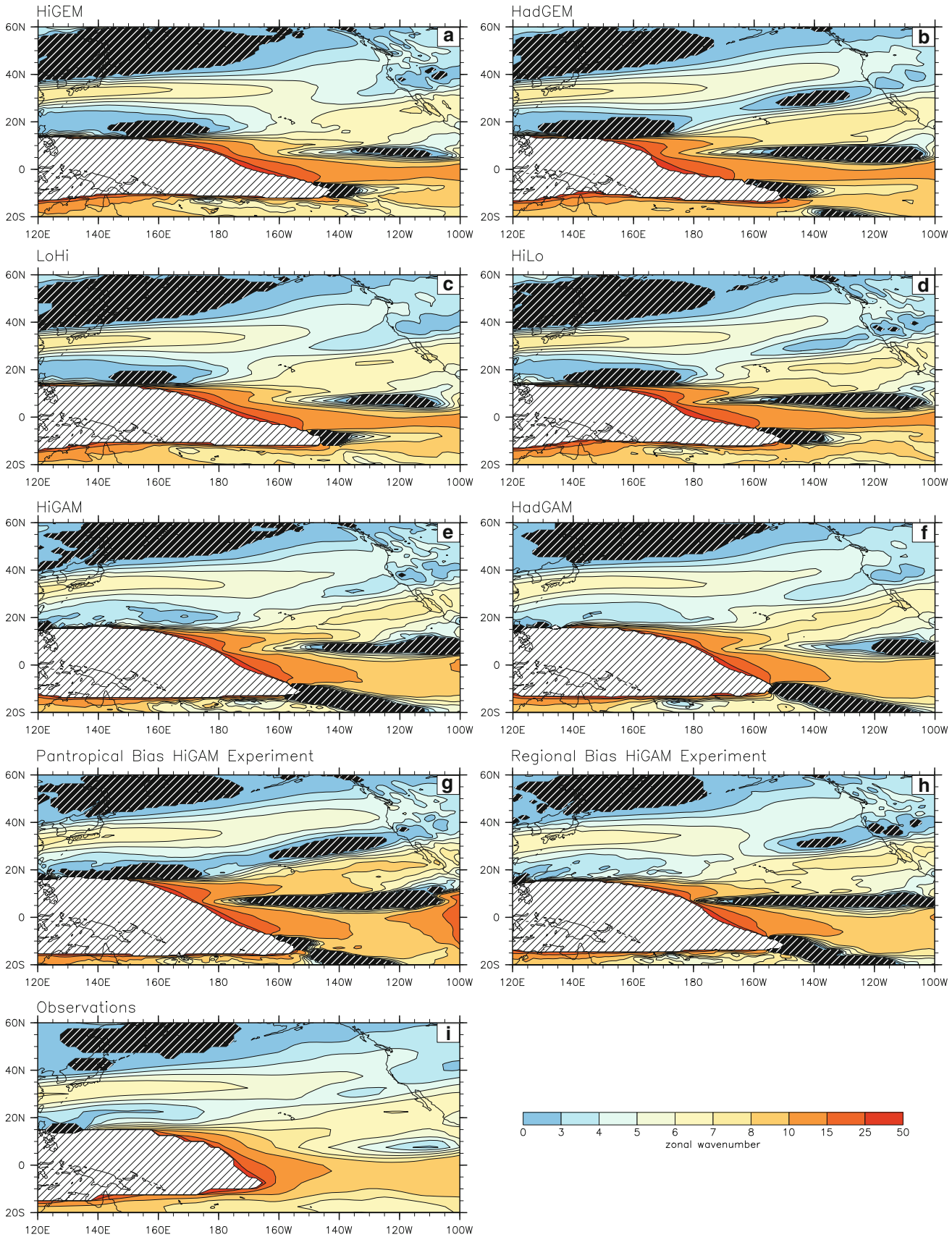
HiGEM
a
HadGEM
b
LoHi
c
HiLo
d
HiGAM
e
HadGAM
f
Pantropical Bias HiGAM Experiment
g
Regional Bias HiGAM Experiment
h
Observations
i
60N
40N
20N
0
20S
120E
140E
160E
180
160W
140W
120W
100W
0 3 4 5 6 7 8 10 15 25 50
zonal wavenumber

◀ **Fig. 2** Zonal stationary wavenumber computed from northern winter (NDJFM) time-mean zonal wind at 200 hPa. Light (*dark*) hatching indicates areas where $\bar{u}$ (β_*) is negative. **a** HiGEM, **b** HadGEM, **c** LoHi, **d** HiLo, **e** HiGAM, **f** HadGAM, **g** pantropical bias HiGAM experiment, **h** regional bias HiGAM experiment, and **i** observations (NCEP/NCAR reanalysis)

HiLo configuration (Fig. 2d) is dynamically similar to that in HadGEM, with an area of very low zonal wavenumber between the two waveguides at 30°N, 140°W. Although there is no actual reversal of the meridional absolute vorticity gradient as in HadGEM, this area of low zonal wavenumber has a similar dynamical effect of being a barrier to Rossby wave propagation. As shown in Fig. 1d, Rossby waves are propagated unrealistically in the HiLo configuration, and this is likely to be due to the more separated structure of the waveguides over the North Pacific. Again, the conclusion from the cross-resolution GCMs is that the improvement in terms of the atmospheric basic state over HadGEM made by increased atmospheric resolution is less than that made by increased oceanic resolution.

Both HiGAM and HadGAM atmosphere-only configurations (Fig. 2e, f) have an atmospheric basic state similar to observations. Critically the basic state in the atmospheric components are similar to one another. This again suggests that insufficient horizontal resolution in the atmospheric model component is not the cause of the erroneous atmospheric basic state in the low resolution coupled model.

3.3 North Pacific sea surface temperature component of El Niño

The surface response in the extra-tropics in now examined. This will provide understanding of how the previously discussed atmospheric mechanisms impact the surface.

The leading EOF (EOF 1) of NDJFM North Pacific SST for HiGEM (Fig. 3a) is similar to EOF 1 for observations

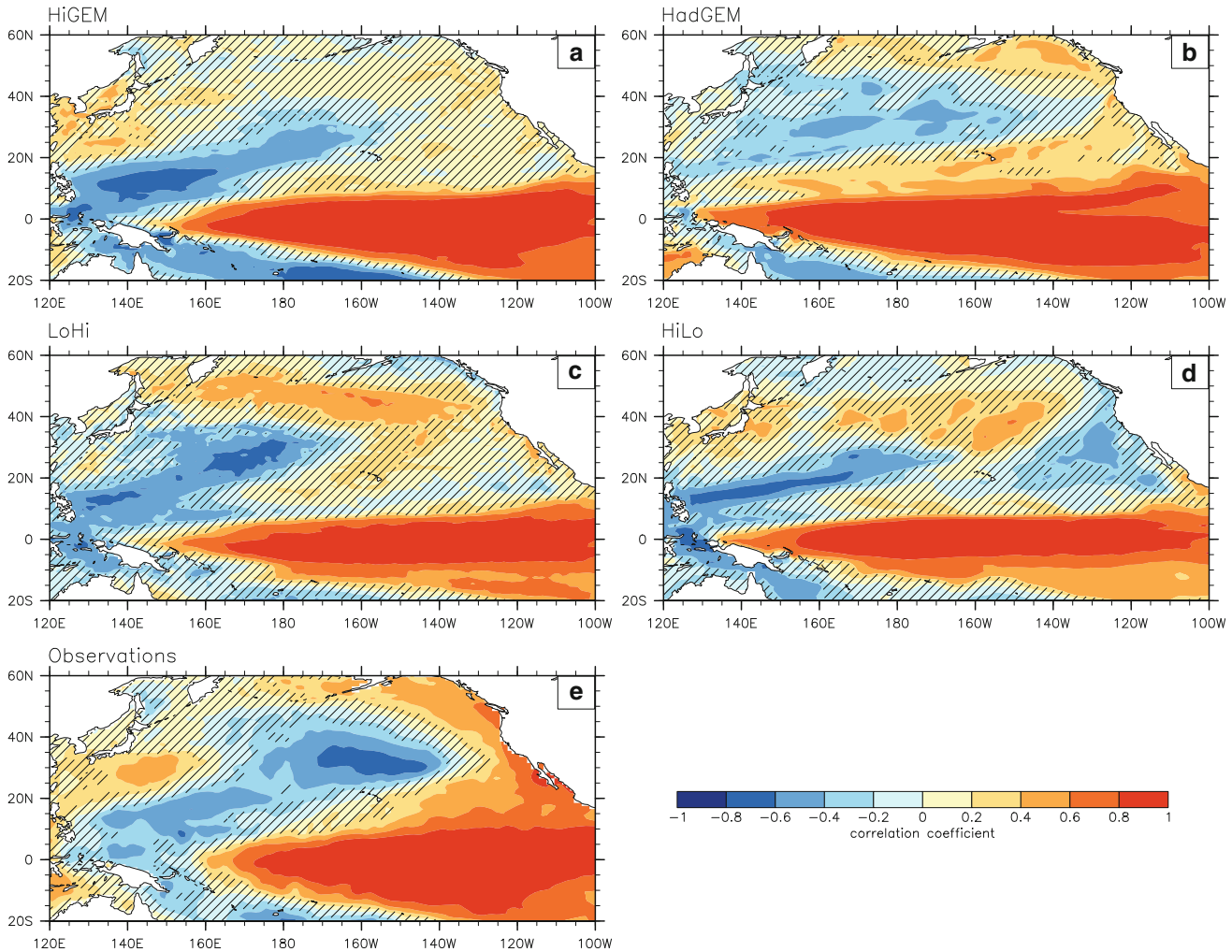

Fig. 3 EOF 1 of northern winter (NDJFM) Pacific SST anomaly normalized by correlation. Correlations that do not pass the 95 % significance level are hatched. Contour interval is 0.2. **a** HiGEM, **b** HadGEM, **c** LoHi, **d** h HiLo, **e** observations (HadISST)

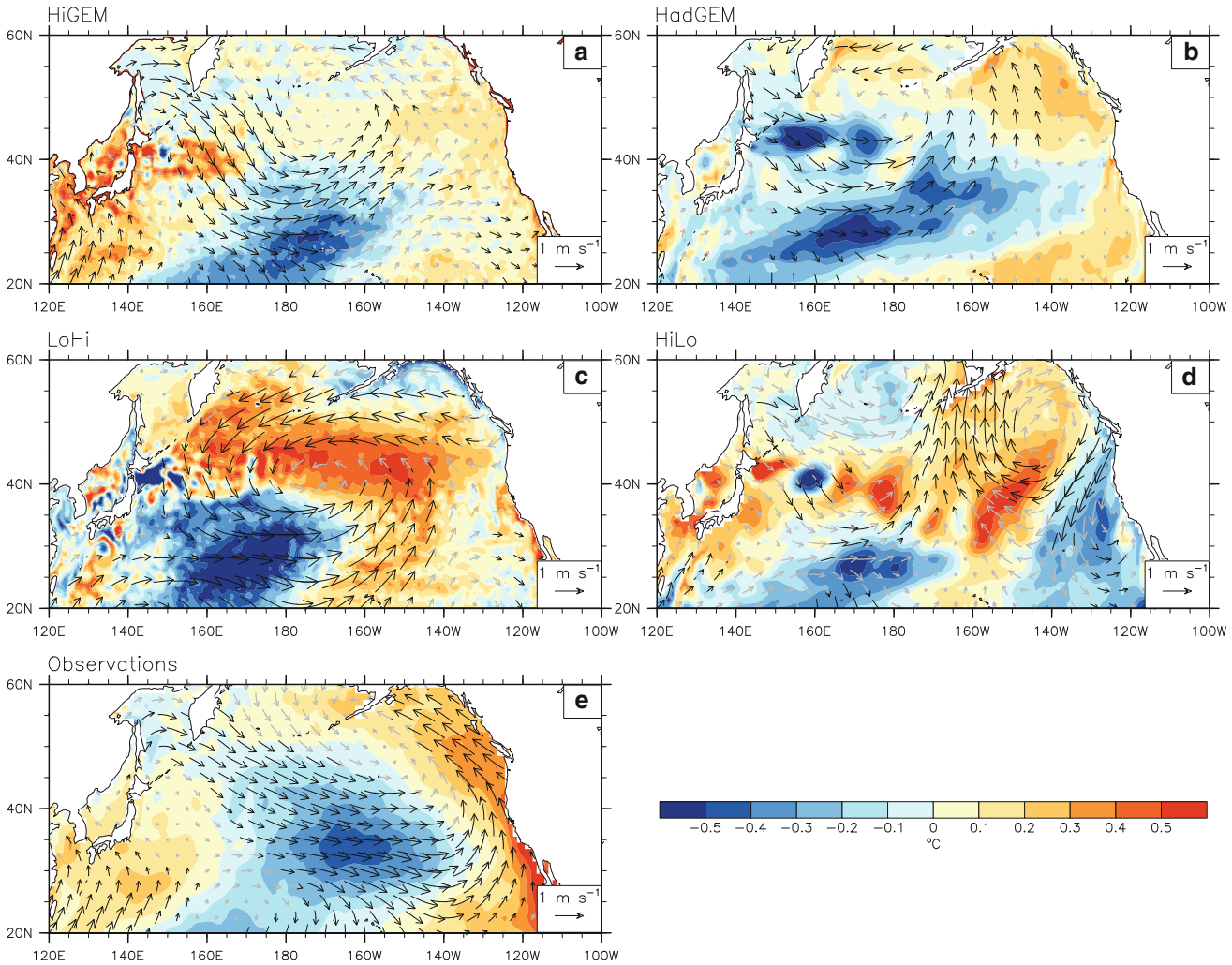

Fig. 4 Northern winter (NDJFM) anomalous SST (*colors*, °C) and surface vector wind (*arrows*, m s^{-1}) regression maps associated with a 1 °C departure of the EP index. Contour interval is 0.1 °C. Surface wind *arrows* for regressions that pass the 95 % significance level are coloured *black*, *arrows* for regressions that do not pass the 95 % significance level are *coloured grey*. **a** HiGEM, **b** HadGEM, **c** LoHi, **d** HiLo, **e** observations (HadISST and NCEP/NCAR reanalysis)

(Fig. 3e), with positive SST anomalies over the equatorial central and eastern Pacific, and a "horseshoe" of negative SST that extends eastwards and polewards into both hemispheres from the equatorial western Pacific. However, HiGEM does not show statistically significant warming along the North American coast. This is likely a consequence of the weaker than observed circulation anomaly over the North Pacific (Fig. 1a). Although the warm anomaly along the North American coast is not statistically significant, it is physically consistent with the surface winds in this region (Fig. 4a) advecting warmer air from the south and warming the sea surface through sensible and latent heat flux anomalies (Dawson et al. 2011), suggesting that they may indeed be real features.

The tropical warm anomaly in both HiGEM and HadGEM (Fig. 3b) extend considerably further westward across the Pacific than observed, which is a common feature of many coupled climate models (Randall et al. 2007). HadGEM also shows an erroneous secondary band of warm anomaly stretching across the Pacific from east to west north of the equatorial warming. This feature is statistically significant and has a large spatial extent. HadGEM is also lacking the the warm anomaly in the western Pacific between 20°–40°N.

HadGEM is producing a statistically significant warm anomaly along the North American coast, a feature of the observations that HiGEM is lacking. We note that the westward shift in upper tropospheric circulation anomaly is also present at the surface in HadGEM (Fig. 4b). It is likely that the influence of this feature in the north-east Pacific, north of 40°N, is to produce the warm anomaly through advection of warmer air from the south. However, the warm anomalies along the North American coast south of 40° north cannot be explained in this manner. In

observations this region is dominated by surface wind driven forcing. In HadGEM the surface wind anomaly here is near zero. It seems more likely that this warm anomaly in HadGEM is actually part of the erroneous secondary off-equatorial warm anomaly noted previously. This suggests that whilst the extra-tropical SST pattern in HadGEM appears realistic near the North American coast, it is due to an erroneous mechanism, and can therefore be considered erroneous.

The tropical component of EOF 1 in the LoHi configuration (Fig. 3c) is similar to that in HiGEM, likely because they use the same oceanic component. An equivalent comparison can be made for the HiLo configuration (Fig. 3d) and HadGEM. In the extra-tropics neither of the cross-coupled configurations are particularly similar to observations. The surface circulation anomaly in LoHi (Fig. 4c) is shifted to the south and lacks the tilt seen in observations (Fig. 4e). This results in the unrealistic extra-tropical SST anomalies, even though the large scale structure (an enhanced low over the North Pacific) is reasonably well replicated. As expected from analysis of upper tropospheric circulation anomalies, the surface wind anomalies in HiLo (Fig. 4d) are completely different from observations resulting in the erroneous extra-tropical SST response.

4 Sensitivity of the atmospheric basic state to systematic SST biases

In Sect. 3 it was demonstrated that the atmospheric basic state in a coupled model, the key ingredient to a realistic representation of the extra-tropical response to El Niño, is significantly improved with increased oceanic resolution, while the improvement due to increased atmospheric resolution is not as pronounced. It was also shown that there is no limitation in the low resolution atmospheric component that prevents it from representing the extra-tropical response to El Niño realistically. It is reasonable to assume that the mean state of the atmosphere is heavily dependent on the mean state of the ocean. Therefore, a sensible place to start looking to understand differences in the atmospheric basic state between HiGEM and HadGEM is the oceanic mean state.

4.1 Winter SST biases

Both HiGEM and HadGEM have a cold SST bias in winter in the north-west Pacific (Fig. 5a, b). A cold SST bias in this region is noted in the climatological annual mean of many coupled models (Randall et al. 2007). Both HiGEM and HadGEM also have a cold SST bias in the North Atlantic. The bias is stronger and covers a greater area in HadGEM than in HiGEM. This cold bias is an effect of the models having insufficient resolution to correctly position the Gulf Stream and North Atlantic Current, and the large SST gradients there. HiGEM has a smaller cold bias in the North Atlantic since its higher oceanic resolution allows a better representation of the orientation of the Gulf Stream than in HadGEM. This particular type of model error is found in many coupled models, as discussed in Randall et al. (2007). Globally, HadGEM has a stronger cold bias than HiGEM (Fig. 5c). On a more regional scale, HadGEM has a strong cold SST bias in the eastern sub-tropical Pacific centred at 20°N, 140°W. This region is local to the extra-tropical wavetrain response to El Niño, that exhibited significant differences between HiGEM and HadGEM. This winter time SST bias is not as marked in HiGEM, and hence could be one of the factors causing the representation of the atmospheric basic state in HadGEM to be inaccurate.

4.2 Perturbation experiments

Two perturbation experiments are set up using the high resolution atmospheric component HiGAM. The aim of this is to attempt to reproduce the erroneous atmospheric basic state seen in HadGEM in the high resolution atmospheric model component by perturbing only the SST boundary condition. Doing so would demonstrate that a better representation of the oceanic component is the important factor needed to accurately simulate the atmospheric basic state, and hence the extra-tropical response to El Niño in a coupled model.

4.2.1 Pantropical bias HiGAM experiment

The first experiment aims to determine if the additional (cold) SST bias that is present in HadGEM but not in HiGEM (Fig. 5c) could be responsible for the unrealistic HadGEM atmospheric basic state. In this experiment the high resolution atmospheric model component is forced with observed SSTs plus the HadGEM minus HiGEM mean northern winter (NDJFM) SST. The latitudinal extent of the imposed bias is limited to 40° north and south (dashed lines in Fig. 5c), to avoid adjusting SST in ice covered regions. This is a reasonable strategy since most of the oceanic forcing of the atmosphere will take place in the tropics and sub-tropics (Graham et al. 1994; Lau and Nath 1994). This experiment is referred to as the pantropical bias HiGAM experiment.

4.2.2 Regional bias HiGAM experiment

The second experiment aims to understand the effect of a more localised SST bias on the atmospheric basic state. Here, the atmospheric model component is forced with

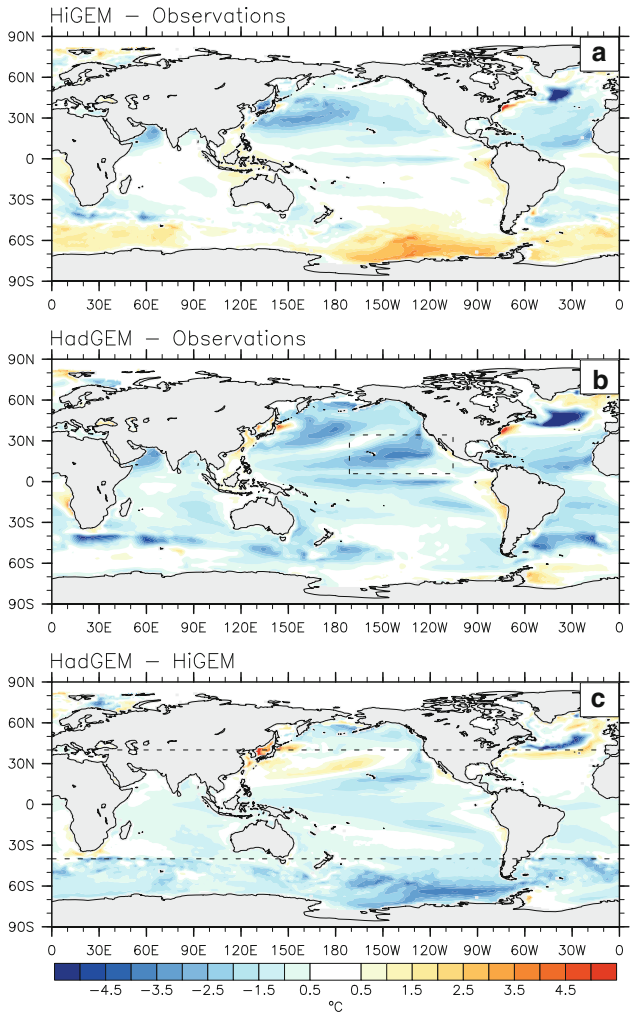

Fig. 5 Differences in northern winter (NDJFM) 50 year time-mean SST for **a** HiGEM minus observations (HadISST), **b** HadGEM minus observations (HadISST) where the *dashed box* indicates the perturbation used for the regional bias experiment, and **c** HadGEM minus HiGEM where the *dashed lines* indicate the boundaries of the perturbation in the pantropical bias experiment. Contour interval is 0.5 °C

observed SSTs plus the HadGEM SST bias centred at 20°N, 135°W (see the dashed area in Fig. 5b). This anomaly is chosen because it is particularly strong, and is not present in HiGEM. Also its position and size correspond approximately to the reversed vorticity gradient separating the downstream portion of the Asian and Pacific waveguides in HadGEM (Fig. 2b). The bias added to the observed SST forcing is the full bias found in HadGEM and not the HadGEM minus HiGEM bias used in the pantropical bias HiGAM experiment. This is because we wish to understand the effect of a specific part of the SST bias from HadGEM, and whether it could be responsible for the split waveguide structure. This experiment is referred to as the regional bias HiGAM experiment.

4.3 Atmospheric basic state

The diagnostic framework used in Sect. 3 is now used to assess the impact of the imposed SST biases on the atmospheric basic state. The waveguide structure in the pantropical bias HiGAM experiment (Fig. 2g) is significantly different from that in HiGAM (Fig. 2e) and observations (Fig. 2i). The Asian jet waveguide and North American jet waveguides are distinctly separate structures. They are separated by regions of reversed absolute vorticity gradient (dark hatching) over the eastern and western Pacific. This waveguide structure is similar to that in HadGEM (Fig. 2b).

In the regional bias HiGAM experiment (Fig. 2h) there is also an area of reversed meridional vorticity gradient (dark hatching) over the eastern Pacific, separating the waveguides associated with the Asian and North American jets. Again, this separation is characteristic of the HadGEM atmospheric basic state. However, over the western Pacific the basic state appears to be similar to that in HiGAM. The major dynamical difference between the HiGEM and HadGEM basic states is that waves are easily able to cross between waveguides in HiGEM and not in HadGEM. Whilst Rossby waves will be partially blocked from crossing between waveguides by the area of reversed vorticity gradient, this region is much smaller than in the pantropical bias HiGAM experiment (Fig. 2e), and Rossby waves are likely to be able to cross between the two waveguides to the west of this region. Hence, the imposed regional SST bias has an isolated effect on the basic state structure, only altering a portion between waveguides downstream of the wave selection region. This suggests that the the dynamics of the regional bias HiGAM experiment, and hence the atmospheric bridge mechanism that controls the extra-tropical response to El Niño, are likely to be similar to those in HiGAM, although there may be different responses downstream of the SST perturbation.

4.4 Upper tropospheric response

The vorticity response to El Niño (positive vorticity anomaly over central North America, negative anomaly over Canada, positive anomaly over the North Pacific) in the pantropical bias HiGAM experiment (Fig. 1g) is weaker and shifted westward relative to HiGAM (Fig. 1e) and observations (Fig. 1i). These differences in the strength and location of the upper tropospheric anomalies are also noted in HadGEM (Fig. 1b) and are ultimately responsible for the erroneous surface circulation and heat flux anomalies that cause extra-tropical SST anomalies as a response to El Niño (Dawson et al. 2011).

Over the Pacific–North American region the vorticity anomalies in the regional bias HiGAM experiment (Fig. 1h)

are much like those in the HiGAM (Fig. 1e) in terms of size, shape, and location. There is a small difference in the way the two positive vorticity anomalies over the North Pacific and North America join, as we might expect from the isolated differences in basic state in that region.

Generally the global atmospheric response in the regional bias HiGAM experiment appears similar to that in HiGAM. It is clear that, aside from these localised effects, there is little difference between the two experiments downstream of the imposed SST bias. Hence it appears that the errors in the upper tropospheric response to El Niño in the low resolution coupled model HadGEM are due to the SST biases in that model over a wide area of the tropics, and not just to local SST biases in the vicinity of the Pacific jets.

4.5 Surface atmospheric response

Upper tropospheric (potential) vorticity anomalies induce a circulation that extends down to the surface in the extra-tropics. Alternatively, the equivalent barotropic structure of extra-tropical circulation features implies that the circulation anomalies present in the upper troposphere will also be present at the surface. As shown by Dawson et al. (2011) it is this (erroneous) surface circulation (Fig. 6) that ultimately controls the extra-tropical response to El Niño.

HiGAM (Fig. 6c) and observations (Fig. 6d) show similar patterns of surface wind anomaly, as would be expected from their similar upper tropospheric vorticity anomalies (Fig. 1e, i). HiGAM has stronger surface wind anomalies than observations in the North Pacific region. Again, this is consistent with the stronger than observed upper tropospheric anomalies in HiGAM. The surface wind anomalies in the pantropical bias HiGAM experiment (Fig. 6a) are considerably weaker than those in HiGAM, with almost no significant anomalies along the North American coast, and particularly in the south eastern portion of the domain. The westward shift of the main centre of upper tropospheric circulation is again evident in the surface wind regression map. The consequences of these erroneous surface wind anomalies in the pantropical bias HiGAM experiment would be an unrealistic representation of the surface heat flux anomalies that drive the extra-tropical SST response to El Niño.

There is little difference between the anomaly patterns from the regional bias HiGAM experiment (Fig. 6b) and HiGAM. The surface wind anomalies are statistically significant in the same locations and have similar strengths across the Pacific domain. There is nothing in the regional bias HiGAM experiment that suggests that any of the physics of the atmospheric bridge mechanism, including the locations of extra-tropical SST anomalies due to El Niño, would be significantly changed due to the presence of the regionally imposed SST bias.

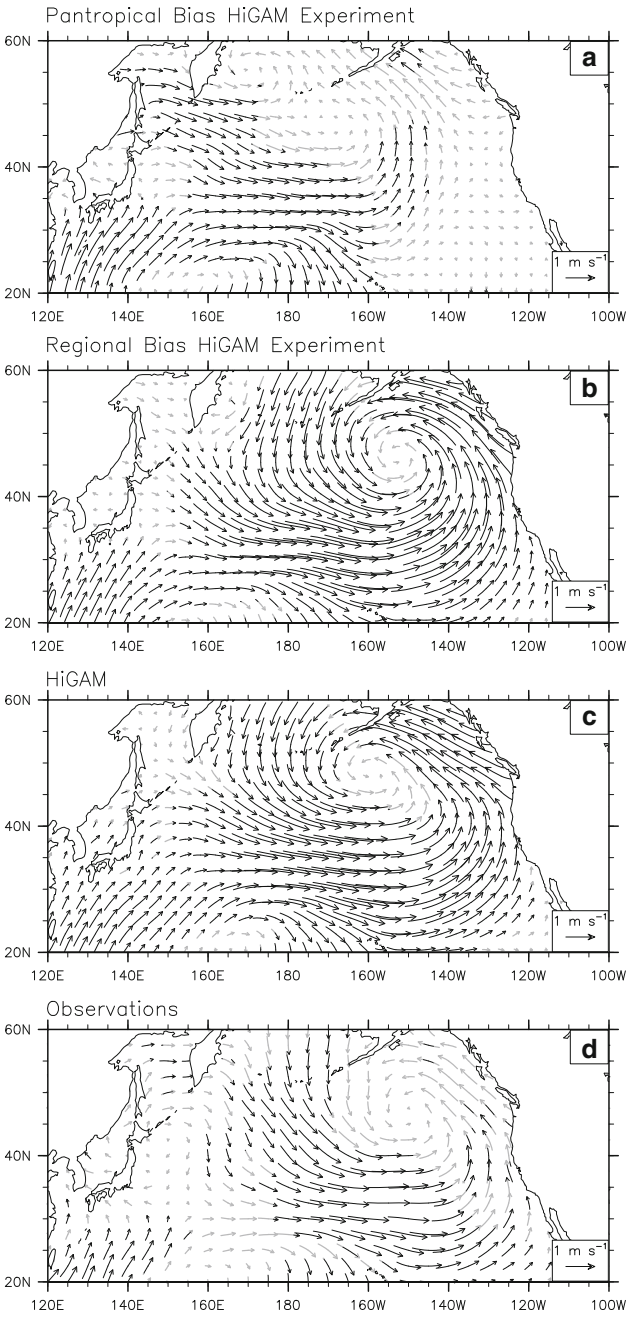

Fig. 6 Northern winter (NDJFM) surface vector wind anomaly associated with a 1 °C departure of the EP index. Surface wind arrows for regressions that pass the 95 % significance level are coloured *black, arrows* for regressions that do not pass the 95 % significance level are coloured *grey*. **a** Pantropical bias experiment, **b** regional bias experiment, **c** HiGAM, and **d** observations (NCEP/NCAR reanalysis) for the 20-year period 1982–2001

5 Conclusions

The effect of horizontal resolution in the atmosphere and ocean on the extra-tropical response to El Niño is examined by diagnosing the atmospheric bridge mechanism in a suite of coupled, atmosphere-only, and cross-resolution

configurations of the UK Met Office coupled climate model. The dynamics of the extra-tropical response to El Niño in the high resolution coupled model HiGEM are similar to the observed dynamics. The teleconnection from the tropics to the extra-tropics in HiGEM is weaker than observed, but the spatial pattern of the response in the extra-tropics is similar to observations.

The atmospheric basic state in the low resolution coupled model HadGEM is erroneous, as was found by Dawson et al. (2011) using a newer version of the model, which causes a less-realistic representation of the extra-tropical response to El Niño. At the surface this error is somewhat masked by apparently compensating errors likely linked to the simulation of tropical El Niño in the oceanic model component.

The atmosphere-only configurations of both the high and low resolution atmospheric components (HiGAM and HadGAM) produce extra-tropical responses to El Niño that are similar to one another and to observations. There is no indication that there is any technical limitation that prevents the low resolution atmospheric component from producing an accurate simulation of the extra-tropical response to El Niño.

When the atmospheric resolution is increased independently of the ocean (HiLo configuration), the extra-tropical SST response is quite poor. The dynamics of Rossby wave generation and propagation, part of the the atmospheric bridge teleconnection mechanism, are unrealistic. The basic state upon which upper tropospheric anomalies propagate is quite different to that of the observed atmosphere. The dynamics of the extra-tropical response to El Niño in the HiLo configuration have much in common with HadGEM, suggesting that an improvement to the atmospheric resolution alone is not sufficient to produce a realistic extra-tropical SST response in the North Pacific.

When the ocean resolution is increased independently of the atmosphere (LoHi configuration), the extra-tropical SST response in the North Pacific does not match particularly well with observations. This seemingly poor response may actually be deceptive. The dynamics of the atmospheric bridge mechanism in the LoHi configuration are actually very similar to HiGEM and observations. The westward shift in the position of upper tropospheric anomalies in HiGEM relative to observations is also present in the LoHi configuration. It is interesting to note that this westward shift is not present in the analysis of Dawson et al. (2011) and perhaps this would also be the case with a cross resolution integration of the later version of HiGEM used in their study. If this were the case then the extra-tropical SST response in the North Pacific could be reproduced well.

When using the higher resolution ocean model coupled to the low resolution atmosphere it is possible to produce a fairly realistic simulation of the extra-tropical response to El Niño. When using the higher resolution atmosphere coupled to the lower resolution ocean this is no longer possible. The best possible performance in terms of the extra-tropical SST response to El Niño is gained from using both high resolution model components. However, the performance gain when moving from low to high atmospheric resolution with a high resolution ocean is much smaller than the performance gain when moving from low to high oceanic resolution with a high resolution atmosphere. The resolution of the ocean model component appears to be more important than the atmospheric resolution in determining the ability of a coupled model system to realistically simulate the extra-tropical response to El Niño.

The performance of the high resolution atmosphere model HiGAM, with respect to the atmospheric bridge mechanism introduced in Sect. 1, in configurations with perturbed SST boundary conditions is also analysed. The aim is to show that with suitable perturbations to the climatological SST boundary conditions, the high resolution atmosphere can be made to reproduce the incorrect atmospheric response to El Niño observed in HadGEM.

When the SST boundary conditions are perturbed so as to impose the pantropical climatological SST difference between HadGEM and HiGEM onto the observed SST forcing, HiGAM produces an unrealistic atmospheric basic state much like that in HadGEM. The atmospheric response to El Niño that propagates on this basic state is considerably different to the response under natural SST forcing. This demonstrates that errors in the SST forcing for HadGAM can be responsible for the incorrect atmospheric basic state. This provides more evidence that it is not atmospheric resolution that is preventing HadGEM from realistically simulating the extra-tropical response to El Niño. A more likely cause is lack of resolution in the ocean, which allows biases in the climatological state of the ocean to be produced, that is in turn responsible for the incorrect atmospheric basic state and poor simulation of extra-tropical response to El Niño in HadGEM.

When a more localised SST bias from HadGEM, one that is not evident in HiGEM, is included in the SST forcing, HiGAM produces a split waveguide structure over the eastern Pacific. However, the main waveguides still merge upstream over the central Pacific, meaning the local splitting effect does not have a significant effect on the overall dynamics of the extra-tropical response to El Niño. Although imposing this specific bias induced a feature in the atmospheric basic state that is similar in some respects to the corresponding feature in HadGEM, it does not appear that an isolated SST bias could cause the majority of the error in the HadGEM basic state. It is more likely that the SST bias on a larger scale is the cause.

It may not be possible to determine which components of the global SST bias are most influential on the atmospheric

basic state. Certainly it is difficult to test this using the same methodology used here. Imposing a global or localised SST bias is relatively straightforward, the former imposes conditions like those in HadGEM and the latter tries to understand a small component of the unrealistic atmospheric basic state. However, imposing multiple or larger scale regional biases would mean there is a good chance of significantly altering the Pacific circulation in such a way that does not happen in HadGEM. For example, imposing an SST bias only in the western Pacific would alter the Walker circulation, introducing significant errors that are not components of the error in HadGEM, but rather are errors due to new physical constraints put upon the system.

This work has shown that the unrealistic atmospheric basic state in HadGEM, which has horizontal resolution typical of the models used in the AR4 climate change assessment, is mainly caused by errors in the oceanic component of the model. When the resolution of the oceanic component is improved as in HiGEM, there is a better representation of the upper ocean and SST in particular. This is likely to be due to the better representation of small scale features in the ocean such as tropical instability waves that flux heat back onto the equator, and the overall reduction in cold tongue bias that results (Roberts et al. 2009). This improvement to the climatological SST allows the atmospheric basic state to develop realistically and hence allows the extra-tropical response to El Niño to occur in a realistic way. This emphasizes a key point in climate modelling, showing that it is critical to simulate the long-term climatological behaviour of the ocean and atmosphere in order to be able to realistically represent short-term climate variability.

Acknowledgments The models described were developed from the Met Office Hadley Centre Model by the UK High-Resolution Modelling (HiGEM) Project and the UK Japan Climate Collaboration (UJCC). HiGEM is supported by a NERC High Resolution Climate Modelling Grant (R8/H12/123). UJCC was supported by the Foreign and Commonwealth Office Global Opportunities Fund, and jointly funded by NERC and the DECC/Defra Met Office Hadley Centre Climate Programme (GA01101). Some model integrations were performed using the Japanese Earth Simulator supercomputer, supported by JAMSTEC. NCEP/NCAR reanalysis data were provided by the NOAA/OAR/ERSL PSD, Boulder Colorado, USA, from their web site at http://www.cdc.noaa.gov/. The UKMO HadISST data were provided by the British Atmospheric Data Centre, from their website at http://badc.nerc.ac.uk/data/hadisst/. AD was supported by a NERC PhD studentship. We thank two anonymous reviewers whose comments helped to improve the manuscript.

References

AchutaRao K, Sperber K (2002) Simulation of the El Niño Southern oscillation: results from the coupled model intercomparison project. Clim Dyn 19(3):191–209. doi:10.1007/s00382-001-0221-9

Alexander MA, Bladé I, Newman M, Lanzante JR, Lau N-C, Scott JD (2002) The atmospheric bridge: the influence of ENSO teleconnections on air–sea interaction over the global oceans. J Clim 15(16):2205–2231. doi:10.1175/1520-0442(2002)015<2205:TABTIO>2.0.CO;2

Brayshaw D, Hoskins B, Blackburn M (2008) The storm-track response to idealized SST perturbations in an aquaplanet GCM. J Atmos Sci 65(9):2842–2860. doi:10.1175/2008JAS2657.1

Brayshaw DJ, Hoskins B, Blackburn M (2011) The basic ingredients of the North Atlantic storm track. Part II: sea surface temperatures. J Atmos Sci 68(8):1784–1805. doi:10.1175/2011JAS3674.1

Dawson A, Matthews AJ, Stevens DP (2011) Rossby wave dynamics of the extra-tropical response to El Niño: importance of the basic state in coupled GCMs. Clim Dyn 37(1):391–405. doi:10.1007/s00382-010-0854-7

Deser C, Blackmon ML (1995) On the relationship between tropical and North Pacific sea surface temperature variations. J Clim 8(6):1677–1680. doi:10.1175/1520-0442(1995)008<1677:OTRBTA>2.0.CO;2

Gordon C, Cooper C, Senior CA, Banks H, Gregory JM, Johns TC, Mitchell JFB, Wood RA (2000) The simulation of SST, sea ice extents and ocean heat transports in a version of the Hadley Centre coupled model without flux adjustments. Clim Dyn 16(2):147–168. doi:10.1007/s003820050010

Graham NE, Barnett TP, Wilde R, Ponater M, Schubert S (1994) On the roles of tropical and midlatitude SSTs in forcing interannual to interdecadal variability in the winter Northern Hemisphere circulation. J Clim 7(9):1416–1441. doi:10.1175/1520-0442(1994)007<1416:OTROTA>2.0.CO;2

Guilyardi E, Gualdi S, Slingo J, Navarra A, Delecluse , J Cole, G Madec, Roberts M, Latif M, Terray L (2004) Representing El Niño in coupled ocean–atmosphere GCMs: the dominant role of the atmospheric component. J Clim 17(24):4623–4629. doi:10.1175/JCLI-3260.1

Hoskins BJ, Ambrizzi T (1993) Rossby wave propagation on a realistic longitudinally varying flow. J Atmos Sci 50(12):1661–1671. doi:10.1175/1520-0469(1993)050<1661:RWPOAR>2.0.CO;2

Hoskins BJ, Karoly DJ (1981) The steady linear response of a spherical atmosphere to thermal and orographic forcing. J Atmos Sci 38(6):1179–1196. doi:10.1175/1520-0469(1981)038<1179:TSLROA>2.0.CO;2

Inatsu M, Mukougawa H, Xie S (2002) Tropical and extratropical SST effects on the midlatitude storm track. J Meteorol Soc Jpn 80(4B):1069–1076. doi:10.2151/jmsj.80.1069

Johns TC, Durman CF, Banks HT, Roberts MJ, McLaren AJ, Ridley JK, Senior CA, Williams KD, Jones A, Rickard GJ, Cusack S, Ingram WJ, Crucifix M, Sexton DMH, Joshi MM, Dong B-W, Spencer H, Hill RSR, Gregory JM, Keen AB, Pardaens AK, Lowe JA, Bodas-Salcedo A, Stark S, Searl Y (2006) The new Hadley Centre climate model (HadGEM1): evaluation of coupled simulations. J Clim 19(7):1327–1353. doi:10.1175/JCLI3712.1

Kalnay E, Kanamitsu M, Kistler R, Collins W, Deaven D, Gandin L, Iredell M, Saha S, White G, Woolen J, Zhu Y, Leetmaa A, Reynolds B, Chelliah M, Ebisuzaki W, Higgins W, Jonowiak J, Mo KC, Ropelewski C, Wang J, Jenne R, Joseph D (1996) The NCEP/NCAR 40-year reanalysis project. Bull Am Meteorol Soc 77(3):437–471. doi:10.1175/1520-0477(1996)077<0437:TNYRP>2.0.CO;2

Karoly D (1983) Rossby wave propagation in a barotropic atmosphere. Dynam Atmos Oceans 7(2):111–125. doi:10.1016/0377-0265(83)90013-1

Kiladis GN, Weickmann KM (1992) Circulation anomalies associated with tropical convection during northern winter. Mon Weather

Rev 120(9):1900–1923. doi:10.1175/1520-0493(1992)120<1900:CAAWTC>2.0.CO;2

Lau N-C, Nath MJ (1994) A modeling study of the relative roles of tropical and extratropical SST anomalies in the variability of the global atmosphere–ocean system. J Clim 7(8):1184–1207. doi:10.1175/1520-0442(1994)007<1184:AMSOTR>2.0.CO;2

Mechoso CR, Robertson AW, Barth N, Davey MK, Delecluse P, Gent PR, Ineson S, Kirtman B, Latif M, Treut HL, Nagai T, Neelin JD, Philander SGH, Polcher J, Schopf PS, Stockdale T, Suarez MJ, Terray L, Thual O, Tribbia JJ (1995) The seasonal cycle over the tropical Pacific in coupled ocean–atmosphere general circulation models. Mon Weather Rev 123(9):2825–2838. doi:10.1175/1520-0493(1995)123<2825:TSCOTT>2.0.CO;2

Navarra A, Gualdi SMS, Behera S, Luo J-J, Masson S, Guilyardi E, Delecluse P, Yamagata T (2008) Atmospheric horizontal resolution affects tropical climate variability in coupled models. J Clim 21(4):730–750. doi:10.1175/2007JCLI1406.1

Norris JR (2000) Interannual and interdecadal variability in the storm track, cloudiness, and sea surface temperature over the summertime North Pacific. J Clim 13(2):422–430. doi:10.1175/1520-0442(2000)013<0422:IAIVIT>2.0.CO;2

Philander SG (1990) El Niño La Niña and the southern oscillation, 1st edn. Academic Press, London, p 287

Philander SGH, Hurlin WJ, Pacanowski RC (1986) Properties of long equatorial waves in models of the seasonal cycle in the tropical Atlantic and Pacific oceans. J Geophys Res 91(C12):14207–14211. doi:10.1029/JC091iC12p14207

Pope V, Stratton R (2002) The processes governing horizontal resolution sensitivity in a climate model. Clim Dyn 19(3):211–236. doi:10.1007/s00382-001-0222-8

Randall DA, Wood RA, Bony S, Colman R, Fichefet T, Fyfe J, Kattsov V, Pitman A, Shukla J, Srinivasan J, Stouffer RJ, Sumi A, Taylor KE (2007) Climate Models and Their Evaluation. In: Solomon S, Qin D, Manning M, Chen Z, Marquis M, Averyt KB, Tignor M, Miller HL (eds) Climate change 2007: the physical science basis. Contribution of working group I to the fourth assessment report of the intergovernmental panel on climate change. Cambridge University Press, Cambridge

Rayner NA, Parker DE, Horton EB, Folland CK, Alexander LV, Rowell DP, Kent EC, Kaplan A (2003) Global analyses of sea surface temperature, sea ice, and night marine air temperature since the late nineteenth century. J Geophys Res 108(D14):4407. doi:10.1029/2002JD002670

Roberts MJ, Banks H, Gedney N, Gregory J, Hill R, Mullerworth S, Pardaens A, Rickard G, Thorpe R, Wood R (2004) Impact of an eddy-permitting ocean resolution on control and climate change simulations with a global coupled GCM. J Clim 17(1):3–20. doi:10.1175/1520-0442(2004)017<0003:IOAEOR>2.0.CO;2

Roberts MJ, Clayton A, Demory M-E, Donners J, Vidale PL, Norton W, Shaffrey L, Stevens DP, Stevens I, Wood RA, Slingo J (2009) Impact of resolution on the tropical Pacific circulation in a matrix of coupled models. J Clim 22(10):2541–2556. doi:10.1175/2008JCLI2537.1

Shaffrey LC, Stevens I, Norton WA, Roberts MJ, Vidale PL, Harle JD, Jrrar A, Stevens DP, Woodage MJ, Demory M-E, Donners J, C D B, Clayton A, Cole JW, Wilson SS, Connolley WM, Davies TM, Iwi AM, Johns TC, King JC, New AL, Slingo JM, Slingo A, Steenman-Clark L, Martin GM (2009) UK-HiGEM: the new UK high resolution global environment model. Model description and basic evaluation. J Clim 22(8):1861–1896. doi:10.1175/2008JCLI2508.1

Wilks DS (2006) Statistical analysis in the atmospheric sciences, 2nd edn. Academic Press, London, p 627